CrystEngComm

Accepted Manuscript

This is an *Accepted Manuscript*, which has been through the Royal Society of Chemistry peer review process and has been accepted for publication.

Accepted Manuscripts are published online shortly after acceptance, before technical editing, formatting and proof reading. Using this free service, authors can make their results available to the community, in citable form, before we publish the edited article. We will replace this *Accepted Manuscript* with the edited and formatted *Advance Article* as soon as it is available.

You can find more information about *Accepted Manuscripts* in the Information for Authors.

Please note that technical editing may introduce minor changes to the text and/or graphics, which may alter content. The journal's standard Terms & Conditions and the Ethical guidelines still apply. In no event shall the Royal Society of Chemistry be held responsible for any errors or omissions in this *Accepted Manuscript* or any consequences arising from the use of any information it contains.

ROYAL SOCIETY OF CHEMISTRY

www.rsc.org/crystengcomm

CrystEngComm RSCPublishing

COMMUNICATION

Bio-inspired Engineering of Zinc Oxide/Amino Acid composite: Synchrotron Microstructure Study

Cite this: DOI: 10.1039/x0xx00000x

Anastasia Brif, Leonid Bloch and Boaz Pokroy*

Received 00th January 2012,
Accepted 00th January 2012

DOI: 10.1039/x0xx00000x

www.rsc.org/

The presence of intracrystalline molecules has been shown to strongly influence crystallite size while at the same time producing strains in both synthetic and biogenic crystals. These molecules, when introduced into ZnO lattice, alter the band-gap energy of the semiconductor. We carry out a high-resolution X-ray microstructure study utilizing synchrotron radiation of bio-inspired ZnO/amino acid composites. Analysis of the adherence profile of the amino acids to the ZnO host is important for achieving better control of the band-gap value of ZnO as a semiconductor.

Materials produced by organisms have continued to attract the interest of researchers over the past decade. This is because of their tremendous potential for improving our understanding of crystal formation and for engineering of new and superior materials. The properties of these materials are expressed in many areas, for example in unique crystal shapes [1], high fracture resistance [2, 3] and altered optical and magnetic properties [4-6]. The micro and macro structures of these crystals have been extensively studied, especially in the case of calcium carbonate [7-9]. Most of the properties of these materials can be attributed to the presence of organic matter within the crystal structure (intracrystalline) and along the grain boundaries of the crystals (intercrystalline). This organic matter consists of unique proteins which can deflect cracks [1], stabilise thermodynamically unstable polymorphs [10, 11], induce crystallisation from amorphous phases [12, 13], and alter the lattice parameters of the crystalline host [14-16]. By employing a bio-inspired approach in which biomineralization-associated proteins are added to the growth solution, these and others crystal properties can be achieved [17-20]. Thus, for example, it was shown that when such proteins become incorporated into synthetic calcite crystals, they alter the crystal morphology and microstructure as compared to control samples [21, 22]. Other molecules, particles, and polymers have also been incorporated within single crystalline hosts of calcite [23, 24]. Surprisingly, the presence of even a single amino acid during synthetic calcium carbonate crystal formation can induce similar results to those seen in their biogenic counterparts [25, 26]. Moreover, latex particles introduced by Wenger et al. into the lattice of ZnO crystals altered the morphology of those non-biogenic crystals as well as their optical and paramagnetic properties [27, 28]. Most recently, our group used this bio-inspired approach to alter the optical and electronic properties of this non-biogenic material [29]. We showed that similarly to the phenomena observed with calcium carbonate [25], a single amino acid became incorporated into the crystal

Department of Materials Science and Engineering and The Russell Berrie Nanotechnology Institute, Technion–Israel Institute of Technology, 32000 Haifa, Israel.
E-mail: bpokroy@technion.ac.il

CrystEngComm Accepted Manuscript

structure of ZnO, causing pronounced lattice strains. The resulting lattice distortion was accompanied by a band-gap energy shift of the ZnO semiconductor host. We found a linear correlation between lattice distortion and the band-gap alternation. After thermal annealing at 300°C for 90 min the band-gap energies returned to their reference values owing to the decomposition of incorporated amino acids. This band-gap relaxation was accompanied by relaxation of the lattice distortion. Similar lattice strain relaxation after annealing has been described in bio-inspired synthetic and biogenic calcite [14-16, 25].

By measuring diffuse reflectance spectra with a Cary 5000 UV-spectrophotometer and using the Kubelka-Munk method for band-gap estimation [30-32], we screened the band-gap alternation of ZnO/amino acid composites before and after thermal annealing (figure 1). A reference sample was used for comparison. All studied amino acid including serine (Ser), glutamic acid (Glu), lysine (Lys), glycine (Gly), tyrosine (Tyr), tryptophan (Trp), aspartic acid (Asp), cysteine (Cys) and seleno-cysteine (Cys), when incorporated into the ZnO lattice, caused a different band-gap alteration probably because of different lattice strains. After thermal annealing, however, in most tested samples the band-gap returned almost to the value of the reference ZnO (3.28ev), which was consistent with previously reported values of 3.2–3.4 eV [33, 34].

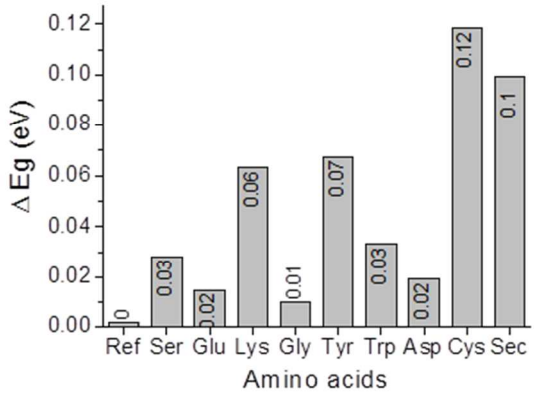

Figure 1: *Band-gap alternation before and after thermal annealing for ZnO incorporated with serine (Ser), glutamic acid (Glu), lysine (Lys), glycine (Gly), tyrosine (Tyr), tryptophan (Trp), aspartic acid (Asp), cysteine (Cys) and seleno-cysteine (Cys).*

This finding allows fine band-gap tuning toward the required values and offers an additional fast, low-cost and low-temperature band-gap engineering route [35]. Therefore, deciphering the spatial arrangement of the amino acids within the crystal structure of ZnO, as discussed in this work is an important innovation that could lead to a better understanding of the causes of band-gap variations.

Before discussing the 3D microstructure we should point out an additional and unusual observation from our previous work. After thermal annealing a broadening of the diffraction peaks was measured, which indicated that a unique microstructure had developed owing to the amino acid incorporation [36]. This was the first observation of such a phenomenon in non-carbonate materials. The observed broadening was unlike that of conventional materials, where owing to crystal growth and defect concentrations decrease, the diffraction peaks narrow upon annealing. However, it was consistent with what we have previously observed in biogenic crystals [37]. In the latter case, organic molecules can interact with specific atomic planes, depending on the chemical recognition between the atomic plane and the organic molecule [2]. This recognition is dependent on the atomic composition and the net charge of the side group of the molecule. During the biomineralization process, adherence of organic molecules to specific atomic planes alters the crystal growth in the perpendicular direction, changing the crystallite size of the crystal blocks [38-40].

Berman et al. [2] determined the location of intracrystalline molecules in calcite by measuring the crystallite sizes in different directions and comparing them to those of a synthetic calcite. They assumed, however, that the broadening was wholly attributable to crystallite size and instrumental broadening. Another method utilised in biogenic calcite was to compare the broadening before and after the annealing process and to take into account the contribution of microstrain fluctuations to the diffraction peak broadening [37]. More details of this method are given below. In the case of semiconductor/amino acids composite crystals,

CrystEngComm Accepted Manuscript

 This journal is © The Royal Society of Chemistry 2012

no such microstructure analysis was performed. We believe that understanding the new microstructure of a composite ZnO/amino acid material is the first step in understanding the band-gap alteration of this composite as compared to pure ZnO. Moreover, it is likely to lead to better control over the innovative bio-inspired band-gap engineering process suggested previously by our group [29].

With the aim of determining the planes to which different amino acids adhere, we analysed the position and the width of X-ray diffraction peaks. In this regard, it should be noticed that peak broadening can result from three major contributory factors, instrumental broadening, crystallite size, and microstrain fluctuations. We emphasise that our experimental setup utilizes a crystal monochromator and a crystal analyser; therefore instrumental broadening is neglected in our further discussion. The diffraction profile can be well fitted to a Voigt function, which is a convolution of both Lorentzian and Gaussian functions. Each contribution can then be separated by deconvolution. The crystallite size component contribution to the Lorentzian peak profile is given by $L = 2d\frac{tan\theta_B}{W_L}$, where L is the crystallite size, W_L is the Lorentzian width, d and θ_B are the d-spacing and Bragg angle for the reflection used, respectively. Similarly, the contribution of the microstrain fluctuations is given by $= 2d\frac{\sqrt{W_G^2 - W_I^2}}{4\sqrt{2ln2}tan\theta_B}$, where σ is the average microstrain fluctuation, W_G is the Gaussian width and W_I is the instrumental broadening (neglected in our study). By using a fitting process utilising the Voigt function approach [37] on a single diffraction peak corresponding to a specific crystallographic plane, we found the W_L and the W_G parameters separately and calculated the average crystallite size and microstrain fluctuation of the reference ZnO sample and of ZnO incorporated with studied amino acids, before and after thermal annealing. These amino acids were chosen from the 21 screened in our previous work because they induced the highest lattice distortion, indicating the highest incorporation level. The profile fitting was performed using gnuplot 4.7 interface [41] over the most intense ZnO peaks, corresponding to the crystallographic planes (100), (002), (101), (102) and (110).

From the data presented in figure 2, some interesting results can be observed. In the case of the reference ZnO, noticeable crystallite size growth upon annealing (52% increase) accompanied by a decrease in microstrain fluctuations (71% decrease) can be seen along (002) plane (figure 2b). This reference ZnO sample showed no significant change in crystallite size and microstrain fluctuations upon annealing along any other crystallographic planes (figures 2a–d). This trend coincides with the usual pattern of conventional materials. The change in calculated average crystallite size and microstrain fluctuation, before and after thermal annealing, is presented in figures 2a–e. The numerical values of the crystallite size and the microstrain fluctuations are presented in table S1 and table S2 of the supplementary data respectively. The typical diffraction peaks of ZnO incorporated with serine can be seen in figure 2f. The insert in figure 2f shows an example of the profile fitting of a single diffraction peak. In contrast to the reference ZnO sample, for most examined amino acids and especially in the case of serine incorporation, the biomimetic ZnO crystal behaviour along the (002) plane clearly showed a reduction in crystallite size upon annealing, suggesting an interaction with the basal planes.

In addition, in the case of serine incorporation, the crystallite size of the ZnO crystals clearly showed a major increase compared to the reference sample along all studied crystallographic planes. This increase may suggest that binding of this amino acid to the ZnO surfaces enhances crystal growth and can serve as a route for growing larger single crystals. By analysing the reduction in crystallite size upon annealing, we can speculate that serine, which is a polar hydrophilic molecule, becomes largely incorporated within the crystal, adhering to all analysed planes (homogenously). Based on our previous study on calcite [25], we can assume that the rather small size of serine and its OH-terminated side group allows it to fit well in the lattice of ZnO, and we can also assume that

CrystEngComm Accepted Manuscript

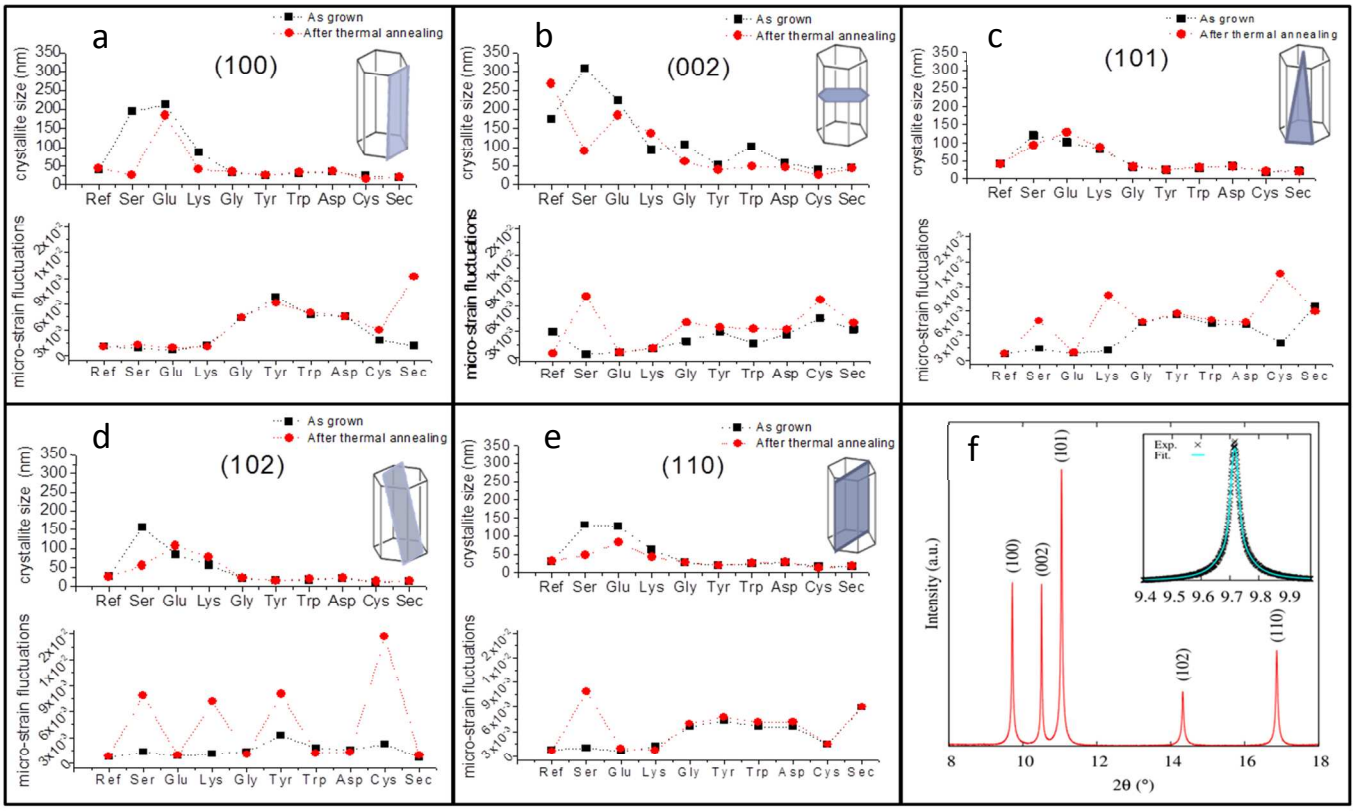

Figure 2: *Crystallite size (nm) and microstrain fluctuations before (black square) and after (red circle) thermal annealing (300°C, 90 min) of reference ZnO and ZnO incorporated with Ser, Glu, Lys, Gly, Tyr, Trp, Asp, Cys, or Sec. Crystallographic planes (a): (100); (b): (002); (c): (101); (d): (102); (e): (110). (f) An example of X-ray diffraction of ZnO incorporated with Ser. On each peak the corresponding crystallographic plane is presented. The insert presents an example of single peak profile fitting.*

probably the hydroxyl group can replace oxygen ions in ZnO.

Analysis of the microstrain fluctuations indicate an increase after annealing in the case of serine incorporation. This result is consistent with the behaviour of biogenic crystals and can be explained by the appearance of new grain boundaries and defects after annealing, owing to destruction of the organic matter within the lattice. As a result, due to the different strain distribution along the newly formed grain boundaries, an increase in the microstrain fluctuations occurs.

Similar to the case of serine, incorporation of glutamic acid resulted in an increase in the crystallite size along most studied planes and a decrease in crystallite size upon thermal annealing. However, annealing was not followed by a significant increase in microstrain fluctuation. This was rather surprising, yet it indicates that after annealing and destruction of the glutamic acid molecules, the lattice of ZnO remained ordered, and no significant new grain boundaries appeared. Microstrain fluctuations have been shown to be strongly affected by the size of the newly formed interfaces [36]. When these interfaces are small, the change in microstrain fluctuations is also expected to be small. This indicates that in the present case the glutamic acid is probably dispersed within the lattice, leaving very small new interfaces when annealed out.

In the case of other analysed amino acids there was no substantial increase in crystallite size compared to the reference sample, and a decrease in crystallite size upon annealing was measured mostly on the (002) plane. This result suggests a specific interaction with the basal planes of ZnO. In the hexagonal Wurtzite crystal structure the basal planes are polar, and it is therefore more likely that amino acids will adhere to them, causing significant lattice strain. Analysis of the microstrain fluctuations after annealing of the (002)

CrystEngComm Accepted Manuscript

This journal is © The Royal Society of Chemistry 2012

plane indicated, as expected, a slight increase. In the case of cysteine interaction with (102) and (101) planes and selenocysteine interaction with (100) plane it can be noticed that although the crystallite size reduction was not significant, a major increase in microstrain fluctuations was measured (figure 2c, d). Such behaviour is typically observed in the case of point defects [36]. We believe that the incorporation of these two amino acids into the ZnO crystal lattice occurs in a different manner from that of the other amino acids tested. They might actually bind via their sulphur and selenium atoms by substitution of these atoms for oxygen and zinc respectively. Once annealed, a point defect remains, which contributes to an increase in the microstrain fluctuations but not to the crystallite size.

The change in average crystallite size along (002) upon annealing, the lattice strain along c-axis and the difference in band gap values before and after annealing for the different amino acid cases is summarized in table S3 of the supplementary data.

Recently, Nawrocki & Cieplak, using molecular dynamics simulations (MD) combined with the umbrella sampling technique, calculated the binding energy ε of common amino acids to four crystal planes of ZnO in aquatic environment [42]. According to their results, the highest ε values for most of the tested amino acids were found along both basal planes of the hexagonal ZnO. Those results are consistent with our finding that most of the tested amino acids interacted strongly with the basal planes of the hexagonal lattice structure. In order to compare our amino acid binding profile to the MD simulation results, we defined the parameter F, corresponding to the "binding fraction" of the amino acid to a specific crystallographic plane. For the amino acids discussed above, the highest binding energy according to MD simulation results was defined as 1, and the other binding energies were normalised to the highest binding energy in order to determine the theoretical F parameter as follows: $F_{th} = \frac{\varepsilon_n}{\max(\varepsilon)}$,where *n* = Ser, Glu, Lys, Gly, Tyr, Trp, Asp or Cys. The data from both basal planes were summarised and compared to the (002) plane in our results. In the case of our experimental data, the relative reduction in crystallite size after thermal annealing, compared to that of the reference sample, resembles the binding energy parameter. The largest relative reduction in crystallite size was defined as 1 (binding of serine to (002) plane) and the other relative crystallite size reductions were normalised by this value to define the experimental F parameter, as follows:

$$\mathrm{F_{exp}} = \frac{(\mathrm{L_{300^oC}-L_{25^oC}})_\mathrm{n}}{(\mathrm{L_{25^oC}})_\mathrm{n}} \backslash \frac{\max(\mathrm{L_{300^oC}-L_{25^oC}})}{(\mathrm{L_{25^oC}})_{\max}}.$$

The comparison between F_{th} and F_{exp} is presented in figure 3. it can be seen from this figure that most of the examined amino acids interacted with the ZnO crystals in a similar way to that predicted by the MD simulation model. For most amino acids, the strongest interaction is along the (002) plane and for the case of serine, homogenous adherence to all analysed planes is noticed both in the MD simulation and in the experimental results. From figure 3 it can be clearly seen, however, that cysteine becomes incorporated significantly stronger than predicted by the theoretical model but in the same interaction manner.

This result may indicate that in contrast to the interactions taken into account in the MD simulation paper [42]., here a stronger chemical interaction between the sulphur atom of cysteine and Zinc atoms exists along the different crystallographic planes (strong thiol-metal bond). In the case of lysine incorporation, the strongest interaction noticed with (110) plane apart from that suggested by the MD simulation. This can be explained by the fact that lysine was the only positively charged amino acid tested and therefore presented a different pattern of interaction. In addition, our experimental results demonstrated slightly lower interaction with the non-polar (100) plane in the case of glycine and tryptophan and the polar (002) plane for the case of glutamic acid. This suggests that additional parameters can influence the interaction profile and should be added to the simulation model such as local pH variations in the crystallization solution, or the probability of developing a protein-like structure by self-assembly of several amino acid molecules in the solution.

CrystEngComm Accepted Manuscript

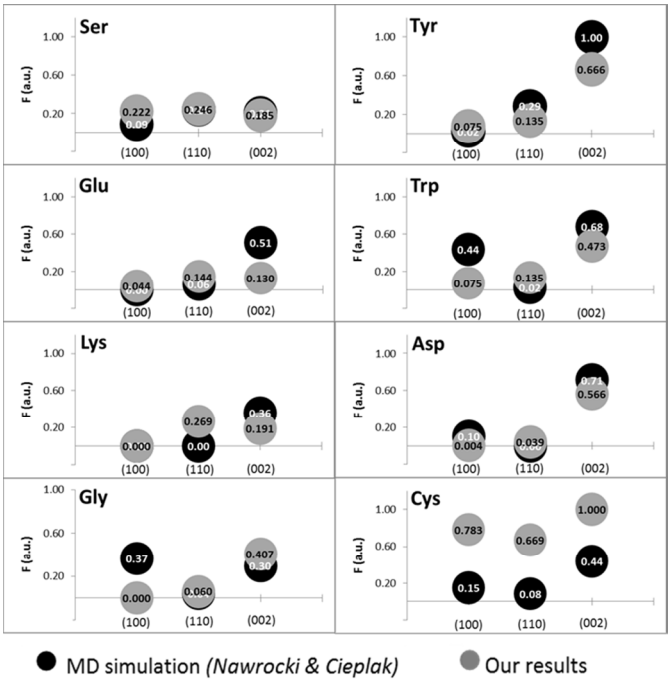

Figure 3: *Comparison between theoretical binding fraction F_{th} based on Nawrocki & Cieplak* [42] *(in black) and our experimental binding fracture F_{exp} (in gray) of amino acids to ZnO crystallographic planes (100), (110), and (002).*

Nevertheless, our experimental results show a good correlation with the MD simulation model, and this model successfully tracks the interaction profile along the different crystallographic planes.

Conclusions

In conclusion, we were able to study not only the lattice strains induced by different amino acids on the ZnO crystallite host and the change in band-gap but also the effects of such molecules on the microstructure. Evolution of the microstructure upon annealing, compared to that of a reference ZnO sample, sheds more light on the manner and pattern of incorporation of the different amino acids. Correlation between the incorporation of specific amino acids and their effect on band-gap shifts is still unclear, and will be the focus of our research in this exciting field in the years to come. Understanding the adherence profile of the amino acids to the ZnO host is an important prerequisite for gaining better control of the band-gap value of ZnO as a semiconductor.

Experimental section

ZnO crystals were crystallised from 0.25 M zinc nitrate hexahydrate (Scharlau Chemie, Spain) and 24%–30% w/w ammonium hydroxide solution (Bio-Lab, Israel) in the presence of 21 amino acids (Sigma-Aldrich) at concentrations ranging from 0.3 to 6 mg/ml. Crystallisation was performed in a round flask, immersed in a silicon oil bath at 95°C for 1 h with constant stirring. The resulting ZnO powders were washed several times with deionised water and then air-dried. Reference ZnO samples were prepared in the same way but without amino acids. Thermal air annealing was performed at 300°C for 90 min.

The X-ray powder diffractions described in this work were measured on beamline ID-31 of the European Synchrotron Radiation Facility (ESRF, Grenoble, France) at a wavelength of 0.476798 Å ± 0.000008 Å. ZnO lattice parameter values were deduced by the Rietveld refinement method (using the GSAS program, EXPGUI interface) and lattice strain was determined as the distortion in lattice parameters compared to the reference ZnO powder.

The optical band gap was established by diffuse reflectance measurements using the Cary 5000 UV–Vis-NIR spectrophotometer (Agilent Technologies) with a DRA-2500 integrating sphere attachment. Optical reflection was obtained over a range of 250 to 800 nm.

Additional information on the experimental methods can be found in our previous work [29].

Acknowledgements

The research that yielded these results received funding from the European Research Council under the European Union's Seventh Framework Program (FP/2013-2018) / ERC Grant Agreement n. [336077]. We thank Maria Koifman for the help in collecting the XRD data at ID31 of the ESRF. We are also indebted to the ESRF (ID31), and specifically to Dr. Christina Drathen and Dr. Andy Fitch, for use and support of the high-resolution powder beamline. We thank Prof. Emil Zolotoybko for helpful discussions.

CrystEngComm Accepted Manuscript

 This journal is © The Royal Society of Chemistry 2012

References

1. J. Aizenberg, N. Ilan, S. Weiner and L. Addadi, Connect Tissue Res, 1996, 35, 17-23.
2. A. Berman, L. Addadi and S. Weiner, Nature, 1988, 331, 546-548.
3. A. A. Chernov, Journal of Structural Biology, 2003, 142, 3-21.
4. A. Levy-Lior, B. Pokroy, B. Levavi-Sivan, L. Leiserowitz, S. Weiner and L. Addadi, Crystal Growth & Design, 2008, 8, 507-511.
5. A. Levy-Lior, E. Shimoni, O. Schwartz, E. Gavish-Regev, D. Oron, G. Oxford, S. Weiner and L. Addadi, Advanced Functional Materials, 2010, 20, 320-329.
6. J. L. Kirschvink and J. L. Gould, Biosystems, 1981, 13, 181-201.
7. P. Fratzl and R. Weinkamer, Progress in Materials Science, 2007, 52, 1263-1334.
8. A. Miserez, J. C. Weaver, P. B. Pedersen, T. Schneeberk, R. T. Hanlon, D. Kisailus and H. Birkedal, Adv Mater, 2009, 21, 401-406.
9. J. C. Weaver, G. W. Milliron, A. Miserez, K. Evans-Lutterodt, S. Herrera, I. Gallana, W. J. Mershon, B. Swanson, P. Zavattieri, E. DiMasi and D. Kisailus, Science, 2012, 336, 1275-1280.
10. Q. L. Feng, G. Pu, Y. Pei, F. Z. Cui, H. D. Li and T. N. Kim, Journal of Crystal Growth, 2000, 216, 459-465.
11. L. Addadi and S. Weiner, Proceedings of the National Academy of Sciences, 1985, 82, 4110-4114.
12. Y. Politi, T. Arad, E. Klein, S. Weiner and L. Addadi, Science, 2004, 306, 1161-1164.
13. L. B. Gower, Chem Rev, 2008, 108, 4551-4627.
14. B. Pokroy, J. P. Quintana. El'ad N. Caspi, Alex Berner and Emil Zolotoyabko, nature materials, 2004, 3, 900-902.
15. B. Pokroy, A. N. Fitch, F. Marin, M. Kapon, N. Adir and E. Zolotoyabko, Journal of Structural Biology, 2006, 155, 96-103.
16. B. Pokroy, A. N. Fitch, P. L. Lee, J. P. Quintana, E. a. N. Caspi and E. Zolotoyabko, Journal of Structural Biology, 2006, 153, 145-150.
17. N. A. J. M. Sommerdijk and G. de With, Chem Rev, 2008, 108, 4499-4550.
18. S. Weiner and L. Addadi, Annu Rev Mater Res, 2011, 41, 21-40.
19. J. W. C. Dunlop and P. Fratzl, Annual Review of Materials Research, Vol 40, 2010, 40, 1-24.
20. L. A. Estroff, Chem Rev, 2008, 108, 4329-4331.
21. Y. Y. Kim, K. Ganesan, P. Yang, A. N. Kulak, S. Borukhin, S. Pechook, L. Ribeiro, R. Kroger, S. J. Eichhorn, S. P. Armes, B. Pokroy and F. C. Meldrum, Nat Mater, 2011, 10, 890-896.
22. Y. Y. Kim, L. Ribeiro, F. Maillot, O. Ward, S. J. Eichhorn and F. C. Meldrum, Adv Mater, 2010, 22, 2082-2086.
23. A. S. Schenk, I. Zlotnikov, B. Pokroy, N. Gierlinger, A. Masic, P. Zaslansky, A. N. Fitch, O. Paris, T. H. Metzger, H. Colfen, P. Fratzl and B. Aichmayer, Advanced Functional Materials, 2012, 22, 4668-4676.
24. H. Y. Li and L. A. Estroff, Adv Mater, 2009, 21, 470-473.
25. S. Borukhin, L. Bloch, T. Radlauer, A. H. Hill, A. N. Fitch and B. Pokroy, Advanced Functional Materials, 2012, 22, 4216-4224.
26. A. Picker, M. Kellermeier, J. Seto, D. Gebauer and H. Colfen, Z Kristallogr, 2012, 227, 744-757.
27. R. Muñoz-Espí, G. Jeschke, I. Lieberwirth, C. M. Gómez and G. Wegner, The Journal of Physical Chemistry B, 2007, 111, 697-707.
28. R. Muñoz-Espí, Y. Qi, I. Lieberwirth, C. M. Gómez and G. Wegner, Chemistry – A European Journal, 2006, 12, 118-129.
29. A. Brif, G. Ankonina, C. Drathen and B. Pokroy, Adv Mater, 2014, 26, 477-481.
30. F. M. P.Kubelka, Z. Tech. Phys., 1931, 12, 593-601.
31. E. L. Simmons, Applied Optics, 1976, 15.
32. R. López and R. Gómez, J Sol-Gel Sci Technol, 2012, 61, 1-7.
33. V. Srikant and D. R. Clarke, Journal of Applied Physics, 1998, 83, 5447-5451.
34. D. C. Reynolds, D. C. Look, B. Jogai, C. W. Litton, G. Cantwell and W. C. Harsch, Phys Rev B, 1999, 60, 2340-2344.
35. F. Capasso, Science, 1987, 235, 172-176.
36. E. Zolotoyabko, J. L. M. Rupp and L. J. Gauckler, Scripta Materialia, 2012, 66, 190-193.
37. B. Pokroy, A. N. Fitch and E. Zolotoyabko, Adv Mater, 2006, 18, 2363-2368.
38. A. Berman, L. Addadi, Å. Kvick, L. Leiserowitz, M. Nelson and S. Weiner, Science, 1990, 250, 664-667.
39. A. Berman, J. Hanson, L. Leiserowitz, T. F. Koetzle, S. Weiner and L. Addadi, Science, 1993, 259, 776-779.

CrystEngComm Accepted Manuscript

40. J. Aizenberg, J. Hanson, T. F. Koetzle, L. Leiserowitz, S. Weiner and L. Addadi, Chem.-Eur. J., 1995, 1, 414-422.
41. T. a. K. Williams, C., Gnuplot 4.7: an interactive plotting program, http://gnuplot.info.
42. G. Nawrocki and M. Cieplak, Physical Chemistry Chemical Physics, 2013, 15, 13628-13636.

CrystEngComm Accepted Manuscript

 This journal is © The Royal Society of Chemistry 2012